



# Benchmarking automotive nonwoven composites from date palm midrib and spadix fibers in comparison to commercial leaf fibers

Lobna A. Elseify<sup>1</sup> · Mohamad Midani<sup>1,2</sup> · Ayman A. El-Badawy<sup>3</sup> · Abdel-Fattah M. Seyam<sup>2</sup> · Mohammad Jawaid<sup>4</sup>

Received: 1 December 2022 / Revised: 24 January 2023 / Accepted: 2 February 2023  
© The Author(s) 2023

## Abstract

In an attempt to increase the biodiversity of natural fibers, new sources of natural fibers should be discovered. Long textile-grade date palm (DP) fibers were used in the manufacturing of 50:50 polypropylene nonwoven composite. DP fibers are considered newcomers to the natural fiber library. The main aim of this work was to benchmark different types of DP fiber composites in comparison to other commercial leaf fiber composites, namely, sisal, abaca, and banana, in addition to Flex-Form automotive composites. The composites were mechanically and physically characterized in order to determine their properties. The results showed that the void content in DP composites was lower than that in sisal and abaca by 33% and 40% respectively. DP composites have tensile strength within the same range as sisal composites and higher than that of banana by nearly 33%. The modulus of elasticity and failure strain of DP composites were nearly 3 GPa and up to 3% respectively. The flexural strength of DP composites (35 MPa) was in the same range as that of sisal and abaca. The normalized impact energy of DP composites was higher than that of banana by 50%. The dynamic mechanical analysis of the six composites showed similar behavior with a glass transition temperature around 10 °C. Finally, the water absorption behavior of DP composites was better than the other composites (lower than sisal by 63%). The results showed that DP fibers are good candidates for applications in automotive interior composites, given their competitive performance and high potential availability.

**Keywords** Date palm fiber · Midrib · Spadix stem · Leaf fibers · Nonwoven composites · Automotive

## 1 Introduction

The automotive industry is one of the major contributors to the greenhouse gas emissions. An average vehicle produces nearly 26.6 tonnes of waste and 922 m<sup>3</sup> of polluted air before being put into use, according to the German Environment and Forecasting Institute. This huge amount of emissions is considered nothing compared to the environmental impact during its life cycle [1]. According to a fact sheet by the International Council

on Clean Transportation, the weight of vehicles is directly correlated to the CO<sub>2</sub> emissions and fuel consumption [2, 3]. There is a global movement to decarbonize the automotive industry to achieve the net-zero goals set forth by many countries. Consequently, the new race in the automotive industry is no longer speed but rather sustainability and light weighting. Natural fiber composites (NFCs) are good candidates for sustainable lightweight vehicles. NFCs are now being used in manufacturing interior auto parts by major car manufacturers such as Mercedes-Benz, BMW, Porsche, and Ford [4–7]. NFCs are used in the manufacturing of door panels, parcel shelves, trunk covers, floor mats, luggage compartments, and ceiling liners [8].

Despite the great progress achieved by original equipment manufacturers (OEM) in incorporating natural fibers in the automotive industry, yet only bast fibers like flax, kenaf, and hemp are being used. The global production of bast fibers is limited and there is a need to explore new sources of vegetable fibers to fulfill the growing demand by the automotive industry.

Vegetable fibers from plant leaves, also known as leaf fibers, represent a good candidate for automotive composites.

✉ Lobna A. Elseify  
lobna.el-seify@guc.edu.eg

<sup>1</sup> Department of Materials Engineering, German University in Cairo, New Cairo, Egypt

<sup>2</sup> Wilson College of Textiles, NC State University, Raleigh, NC, USA

<sup>3</sup> Department of Mechatronics Engineering, German University in Cairo, New Cairo, Egypt

<sup>4</sup> Department of Biocomposite Technology, Institute of Tropical Forestry and Forest Products, Universiti Putra Malaysia, Seri Kembangan, Selangor, Malaysia

The research on leaf fiber composites is very limited compared to that on bast fibers. Several attempts were made to reinforce thermoplastic and thermoset polymers with leaf fibers. The most common leaf fibers are sisal, banana, pineapple, and abaca. They were used with several thermoplastics like polypropylene (PP), polylactic acid (PLA), polybutylene adipate terephthalate (PBAT), and corn starch [9–16]. PP nonwoven composites are manufactured by compression molding or thermoforming. The manufacturing temperature is between 180 and 190 °C [17, 18].

A new emerging source of leaf fibers is the date palm (DP). Fibers could be extracted from the midrib, spadix stem, leaflets, and leaf sheath (mesh) of the palm [19]. In the literature, date palm midrib and spadix fibers were mainly in the form of chopped and milled fibers. DP composites were manufactured by hand lay-up, injection molding, compression molding, and resin transfer molding [20–28]. Several types of polymers were used with DP fibers to manufacture composites. In a study by Refaai et al., they reinforced epoxy with bamboo, DP midrib, spadix stem, and mesh fibers. The composites were manufactured using the hand lay-up method. However, the fibers in this work were very short (0.8–1 mm) [29]. In another research, chemically treated chopped mesh fibers were recently used to reinforce epoxy resin. The results showed that NaOH is better than HCl and CH<sub>3</sub>COOH for fiber treatment to improve the interfacial bond between fibers and matrix [30]. Ghori et al. investigated the properties of 50% wt.% hybrid DP and kenaf epoxy composites. The type of DP fibers in this work was not mentioned and they were in powder form (0.5–1 mm). The composites were manufactured using the hand lay-up technique. The results showed that the treated fibers increased the composite mechanical properties and dimensional stability [31]. The thermal behavior of DP/bamboo fibers was investigated by Jawaid et al. In this study, short (0.8–1 mm) DP fibers extracted from the midrib, spadix stem, mesh, and trunk were used to reinforce epoxy resin. The fibers were in powder form and they could be considered particle. The composite was manufactured using the hand lay-up technique with a 50% fiber weight fraction. The results showed that the addition of DP and bamboo fibers to epoxy has improved the thermal properties of the composites [32]. Another attempt to manufacture DP epoxy composite from DP mesh was made by Ali in 2023. The fibers' length was between 2.5 and 10 mm long and the fiber/matrix mixture was poured into silicon molds. Although the length of fibers in this work is longer than that in other studies, it is still considered short compared to textile-grade fibers. The results showed that increasing the fiber wt.% had a positive effect on the mechanical properties of the composites [33]. The attempts in the literature to extract long fibrillated date palm fibers were not always successful. Most of the previous attempts in the literature were considered wood

plastic composites and not natural fiber composites. Consequently, the composites made from date palm fibers usually had properties lower than the neat polymer since the fibers in this case acted as inclusions [34, 35]. The most DP successful composites were reinforced with mesh fibers since they already exist in the fibrous form [36–38].

By reviewing the work done on DP fibers, it can be concluded that none of the previous attempts succeeded in utilizing long textile fibers in making natural fiber composites that complies with the automotive standards. Hence, the purpose of this research is to develop composite panels from long textile date palm midrib and spadix fibers in a nonwoven structure blended with 50% wt. thermoplastic fibers according to the automotive standards, and to benchmark in comparison to other commercial leaf fiber composites. This article is considered the first attempt to develop and manufacture nonwoven thermoplastic panels from long date palm fibers and to benchmark them against other leaf fiber composites.

## 2 Materials and methods

### 2.1 Materials

The materials used in this work are divided into 2 categories: natural fibers as reinforcement and a polymeric material as a matrix. The natural fibers used were sisal, abaca, banana, date palm midrib (DPM) core and skin, and DP spadix stem fibers. Sisal and abaca fibers were provided by Canal Rope Company located in Port Said, Egypt. Banana fibers were obtained from the “Egypt Foundation for Integrated Development – El Nidaa.” Date palm (DP) fibers were supplied by Valorizen, Egypt, under the trade name PalmFil [39, 40].







Table 1 shows the properties of the fibers used. All natural fibers were cut into 70-mm-long fibers using scissors.

Polypropylene (PP) was used in fiber form as a matrix material, supplied by Egyptex Co. It was chosen specifically due to the faster manufacturing process and better recyclability. PP was in the form of short staple fibers of about 70 mm in length, with a fineness of 17 dtex, a density of 0.91 g/cm<sup>3</sup>, and a melting temperature of about 165 °C.

### 2.2 Composite manufacturing

Six different nonwoven composite samples were prepared, in which each panel is reinforced with a single type of fiber. The composites were made from 50% wt. leaf fiber and 50% wt. PP fiber. This ratio was specifically chosen as per the automotive standards. The high leaf fiber wt.% results in large void content. However, this is desirable in the automotive industry to enhance the thermal and acoustic insulation of the composite at the expense of the mechanical properties.

**Table 1** Average properties of the six natural fibers [41]

Fiber	Equivalent diameter ( $\mu\text{m}$ )	Density ( $\text{gm}/\text{cm}^3$ )	Cellulose (%)	Tensile strength (MPa)	Young's Modulus (GPa)	Failure strain (%)	CrI (%)	Fiber Appearance
Sisal	167.7	$1.33 \pm 0.12$	49.5	777.9	11.67	4.3	59.5	
Abaca	199	$1.58 \pm 0.08$	70.9	946.7	11.4	8.3	69.8	
Banana	121.4	$1.28 \pm 0.09$	57.2	377.5	12.2	3.1	52.4	
DPM Core	131.7	$1.35 \pm 0.01$	52.5	583.5	22.5	2.6	58.5	
DPM Skin	252	$1.35 \pm 0.2$	52.7	393	13.9	2.8	64	
DP Spadix	123	$1.32 \pm 0.21$	59	601.7	19.6	5.1	59.9	

The preforms were made by blending equal weights of natural fibers and PP. The fibers were blended thoroughly to ensure equal distribution of natural fibers. Afterwards, the blended nonwoven fiber webs were laid into a mold with dimensions  $30 \times 30$  cm.

Before composite manufacturing, the fiber preforms were dried for 4 h at  $80^\circ\text{C}$  to remove excess moisture. Afterwards, the composite laminates were prepared by hot pressing. The samples were first pre-heated under 3 MPa for 1 min then hot pressed for 15 min under 15 MPa at  $183^\circ\text{C}$ . The final shapes of the six composites are shown in Fig. 1.

## 2.3 Testing

### 2.3.1 Density and void content

The areal and volumetric densities were calculated for each composite using Eq. (1) and Eq. (2) respectively, where  $m$  is the composite mass,  $A$  is the composite area, and  $v$  is the composite volume. For density calculation, the average of 12 readings was calculated and reported. The void content was calculated using Eq. (3) according to ASTM D2734-16.

$$\text{Areal density (g/m}^2\text{)} = \frac{m}{A} \quad (1)$$

$$\rho_c (\text{kg/m}^3) = \frac{m}{v} \quad (2)$$

$$\text{Void content (\%)} = 1 - \rho_c \left( \frac{1 - w_f}{\rho_m} - \frac{w_f}{\rho_f} \right) \quad (3)$$

where  $\rho_c$  is the composite's densities, while  $\rho_f$ ,  $\rho_m$ ,  $w_f$ , and  $w_m$  are the fiber's density, matrix density, fiber weight fraction, and matrix weight fraction respectively.

### 2.3.2 Tensile properties

The tensile properties were determined according to the standard ASTM D3039/D3039M. Figure 2 shows a schematic diagram of the test. The tests were conducted using ZwickRoell Z100 at a strain rate of 2 mm/min. The sample size was  $24 \times 160$  mm. Six specimens were tested per sample and the average was reported. The fractured surface of the six composites was analyzed using a field emission scanning

**Fig. 1** Composite preparation (left) and manufacturing and final specimens' shape (right)

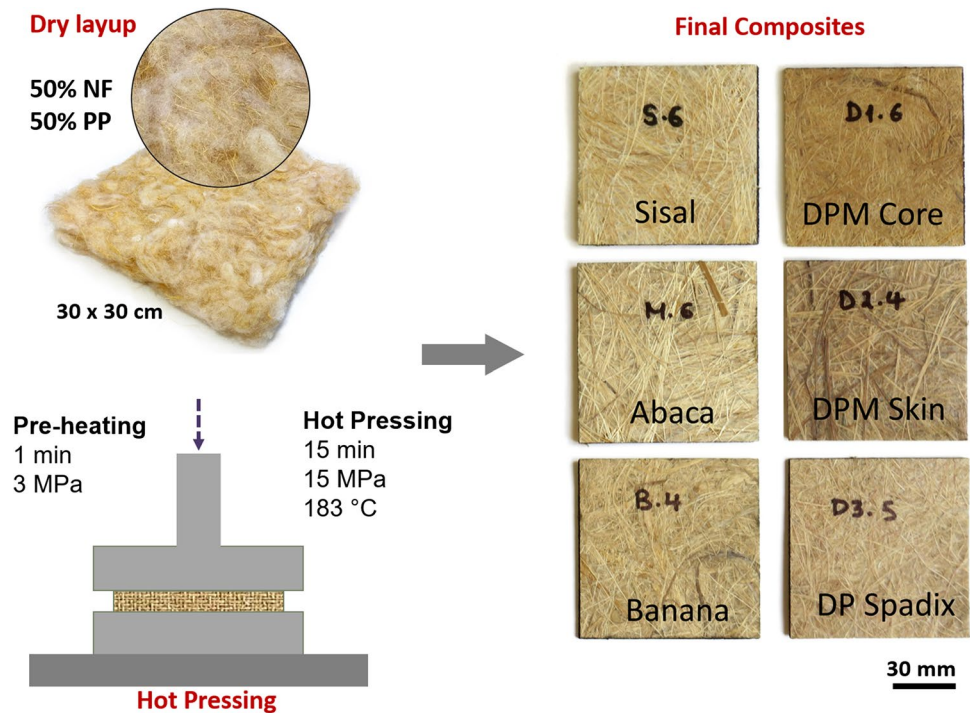
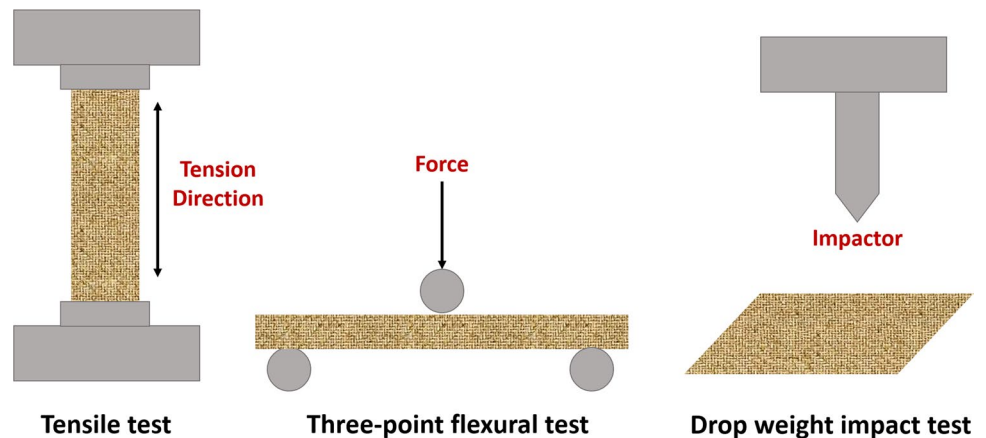


**Fig. 2** Tensile, flexural, and impact test schematic diagrams



electron microscope (FESEM) (Quanta 250 FEG, FIE, Netherlands) with an accelerating voltage of 20 kV.

### 2.3.3 Flexural properties

The flexural properties, using the three-point test, were determined based on the standard test ASTM D7264/D7264M. Figure 2 shows a schematic diagram of the test. The test was conducted using ZwickRoell Z100 at a strain rate of 2 mm/min. The span length was set to be 32 times the specimen's thickness. The average composite thickness was 2 mm; hence, the span length was set to 64 mm. Six specimens were tested per sample. Following the ASTM standard procedures, the flexural chord modulus was calculated using Eq. (4).

$$E = \frac{L^3 m}{4 b h^3} \quad (4)$$

where  $E$  is the flexural modulus in MPa,  $L$  is the span length in mm,  $b$  and  $h$  are the width and thickness of the specimen respectively in mm, and finally,  $m$  is the slope of the force–displacement curve.

### 2.3.4 Impact properties

The impact properties were determined as per the ASTM test number D3762. Figure 2 shows a schematic diagram of the test. Instron Tower Impact CEAST 9350 was used to conduct drop weight impact tests. The specimen was square-shaped

having a side length of 60 mm. Five specimens were tested per sample. The impact velocity was 4.4 m/s with a maximum value of change 20%. The striker had a diameter of 12.7 mm and the specimens were pneumatically clamped during the test.

### 2.3.5 Dynamic mechanical analysis (DMA)

The DMA tests were conducted according to ASTM D4065-01 to determine and compare the viscoelastic properties of the six composites. TA (DMA Q 800) instrument was used for the DMA analysis which operated in a three-point bending mode. The testing was at temperature ranging from -100 to 160 °C under controlled sinusoidal strain at a heating rate of 5 °C/min and a frequency of 1 Hz under controlled amplitude. The specimens' dimensions were 60×12.5×3 mm.

### 2.3.6 Water absorption and moisture content

The water absorption (WA) and moisture content (MC) were determined for the six composites according to the standard test number BS EN 322. The weight of all specimens was measured with an accuracy of 0.01 g. The specimens were in the form of a square having a side length of 3 cm, and 5 specimens were tested per sample. For the water absorption test, the samples were immersed in distilled water at room temperature. The test was conducted for 168 h. The weight was recorded before and after immersion every 24 h. The increase in the specimen's weight was calculated using Eq. (5). As for the moisture content test, the specimens were subjected to 3 drying rounds and each was 6 h long. The drying was at 100±5 °C and the weight was recorded before and after each round. The moisture content was calculated using Eq. (6).

$$WA = \frac{W_{final} - W_{initial}}{W_{initial}} \times 100 \tag{5}$$

$$MC = \frac{W_{initial} - W_{final}}{W_{initial}} \times 100 \tag{6}$$

where  $W_{final}$  and  $W_{initial}$  are the specimen's final and initial weights respectively.

### 2.3.7 Thickness swelling

The composite thickness swelling (TS) was determined according to the standard test BS EN 317. The specimens' thickness was measured before and after water immersion for 24 h. The specimens were immersed in distilled water at room temperature. The test was carried out for 168 h. The specimens were square-shaped with a side length of 3 cm. Thickness swelling was calculated using Eq. (7).

$$TS = \frac{T_{final} - T_{initial}}{T_{initial}} \times 100 \tag{7}$$

where  $T_{final}$  and  $T_{initial}$  are the specimen's average final and initial thickness values respectively.

## 3 Results and discussion

### 3.1 Density and void content

The composite density is a very important parameter in designing lightweight components. The density of the composite is influenced by two main factors: density of constituents (i.e., fiber and matrix) in addition to void content. In designing nonstructural automotive interior composites, it is common to have void content in the range of 30% to increase the thermal and acoustical insulation, even if this will be at the expense of the mechanical performance. The void content also has a direct influence on other performance parameters, such as water absorption, thickness swelling, and vibration damping of the produced composites. Hence, calculating the void content will be important in interpreting all subsequent testing results. The results of the composite densities and void contents are presented in Table 2.

The void content in the composites is resulting from 2 sources: first the voids in the fiber microstructure and second the voids between the fiber and the matrix due to poor wetting and creation of air pockets at the cross-over points between fibers. The voids in the fiber microstructure are either in the form of vascular cavities or lumens, while the voids created between the fiber and the matrix are heavily

**Table 2** Thickness, void content, areal and volumetric densities of the six composites

Fiber	Thickness (mm)	Areal density (gm/m <sup>2</sup> )	Volumetric density (kg/m <sup>3</sup> )	Void content (%)
Sisal	2.7 ± 0.25	1815	680.6 ± 70	36.9 ± 2.2
Abaca	2.6 ± 0.14	1815	690.3 ± 36	40.3 ± 1.02
Banana	1.98 ± 0.20	1488	750.9 ± 87	29.3 ± 2.2
DPM core	2.07 ± 0.06	1694	818 ± 28	24.7 ± 0.1
DPM skin	2.12 ± 0.07	1730	815.8 ± 28	22.1 ± 0.45
DP spadix	1.9 ± 0.12	1597	829.7 ± 59	25.7 ± 0.36

dependent on the fiber's ability to deform and fill the gaps in the structure, which depends on the fiber bending rigidity which is influenced by the fiber diameter.

Abaca composite had the highest void content (40.3%) due to the presence of lumens and due to the large rigid fiber bundles; this was followed by sisal (36.997%) which had smaller fiber bundles but rather had large vascular cavities in addition to existing lumens. Despite that banana fiber bundles had very large lumens and very thin cell walls, yet the fact that they have relatively small diameter resulted in less void content (29.34%) compared to sisal and abaca. As for date palm composites, they had the least void contents (< 26%) due to the small lumen sizes (negligible) and small fiber bundles which were capable of deforming easily and conforming to the structure gaps. All fiber cross-sectional shapes are presented in the SEM micrographs in Fig. 3.

### 3.2 Tensile properties

The most significant factors that affect natural fiber composite strength are the fiber weight fraction, fiber strength, composite defects, and the interfacial bond between fibers and matrix. Voids or air pockets are considered composite defects that appear due to insufficient wettability between matrix and fibers, whereas the interfacial bond between fibers and matrix is affected by the surface impurities, fiber size, and surface roughness.

The typical tensile stress–strain curves and the average tensile properties are shown in Fig. 4a. Figure 4b shows the tensile strength of the composites in the light of the fibers' strength. The tensile strength of the composites followed the same trend as those of the fibers. This was expected since the fiber tensile properties have a high influence on the composite tensile properties. The abaca composite was the toughest composite, and it showed considerably the highest tensile strength among the 6 composites of  $32.13 \pm 4.02$  MPa. This was due to the high strength of fibers in spite of the high void content in the abaca composite. The abaca composite was followed by sisal and date palm spadix composites, which had tensile strength values of  $24.5 \pm 2.78$  MPa and  $23.56 \pm 2.95$  MPa respectively with no statistical significance between the two composites. Additionally, it was noticed that the tensile strength of date palm core and skin midrib composites has nearly the same tensile strength with the midrib core composite having a higher stiffness than that of the midrib skin composite. The tensile strength of midrib core and skin composites was  $21.53 \pm 1.6$  MPa and  $20.3 \pm 1.87$  MPa respectively, which were not consistent with the fibers' strength behavior. This could be attributed to the surface difference between the midrib core and skin fibers. Both date palm midrib core and skin fiber bundles are lined with silica crystals on their outer surface which create mechanical interlocks between the fibers and the matrix as shown in Fig. 5. However, in the case of the midrib core, the

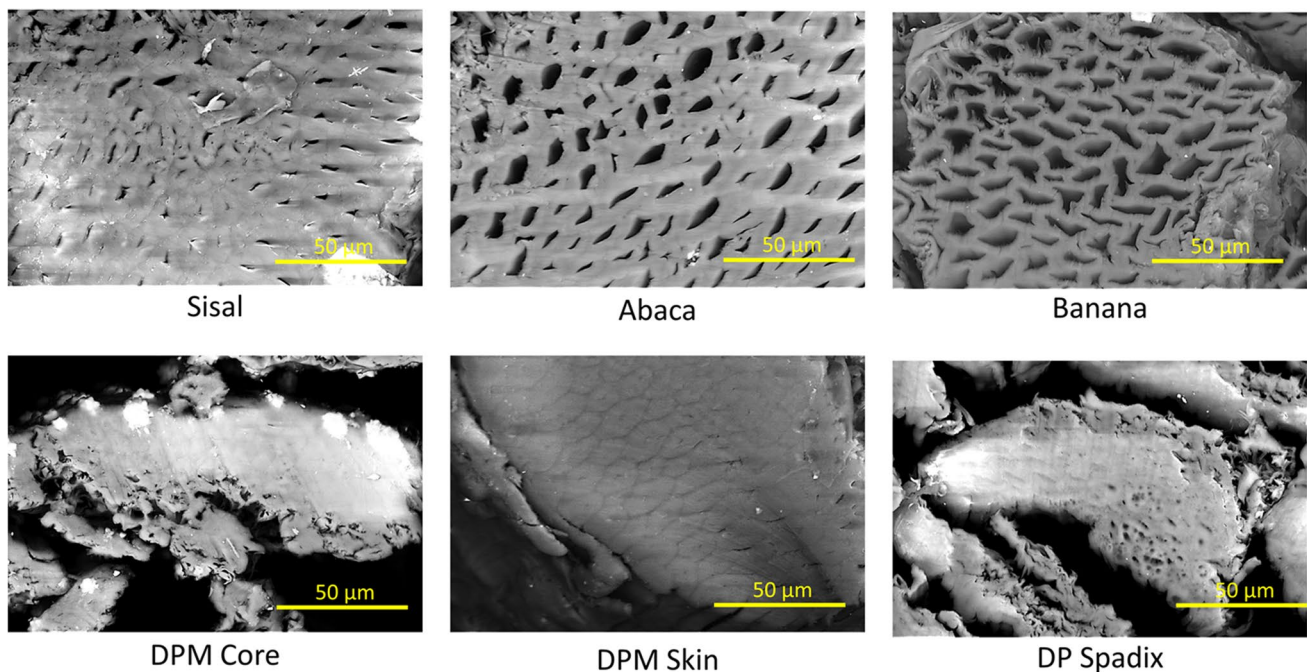
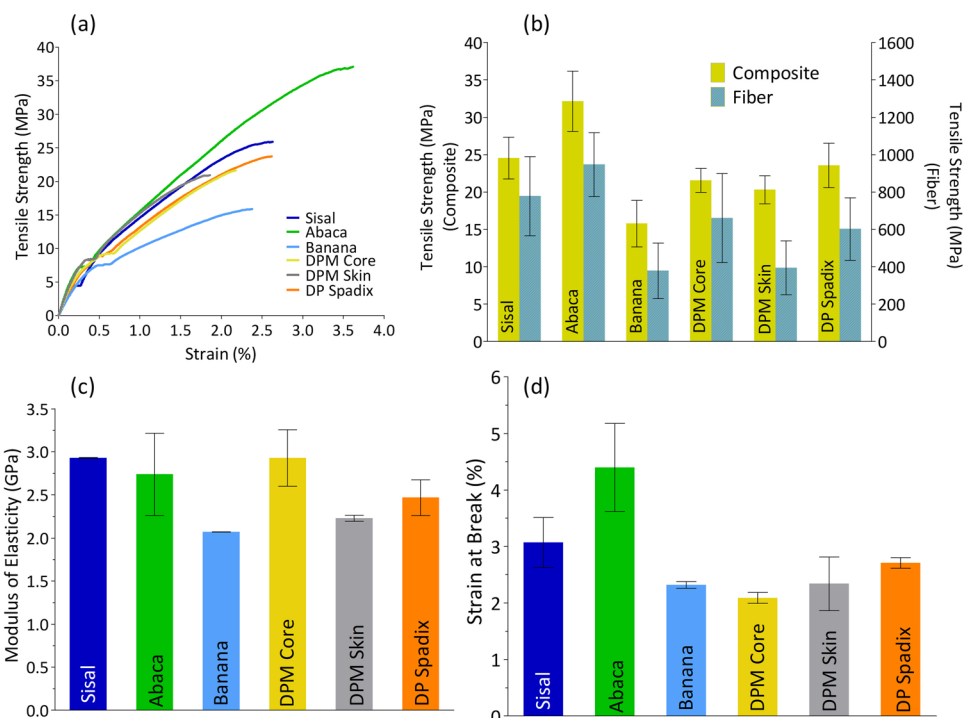


**Fig. 3** SEM micrographs at 2600× magnification showing the cross-section of sisal, abaca, banana, DP midrib core, and skin fibers and DP spadix fibers

**Fig. 4** **a** Typical tensile stress–strain curves and average values of **b** tensile strength, **c** modulus of elasticity, and **d** strain at break of the six samples



bundles are usually used after splitting; hence, the silica crystals will only be lined on one side, which represents a segment of the outer surface, whereas in the case of the midrib skin, the fiber bundles are non-fibrillated, and the entire bundle surface is lined with silica crystals. Thus,

midrib skin composites had enhanced interfacial adhesion due to the circumferential interlocking; furthermore, they had lower void content which led to enhanced behavior. Although the tensile strength of sisal fibers was higher than that of date palm fibers, as shown in Fig. 4b, their

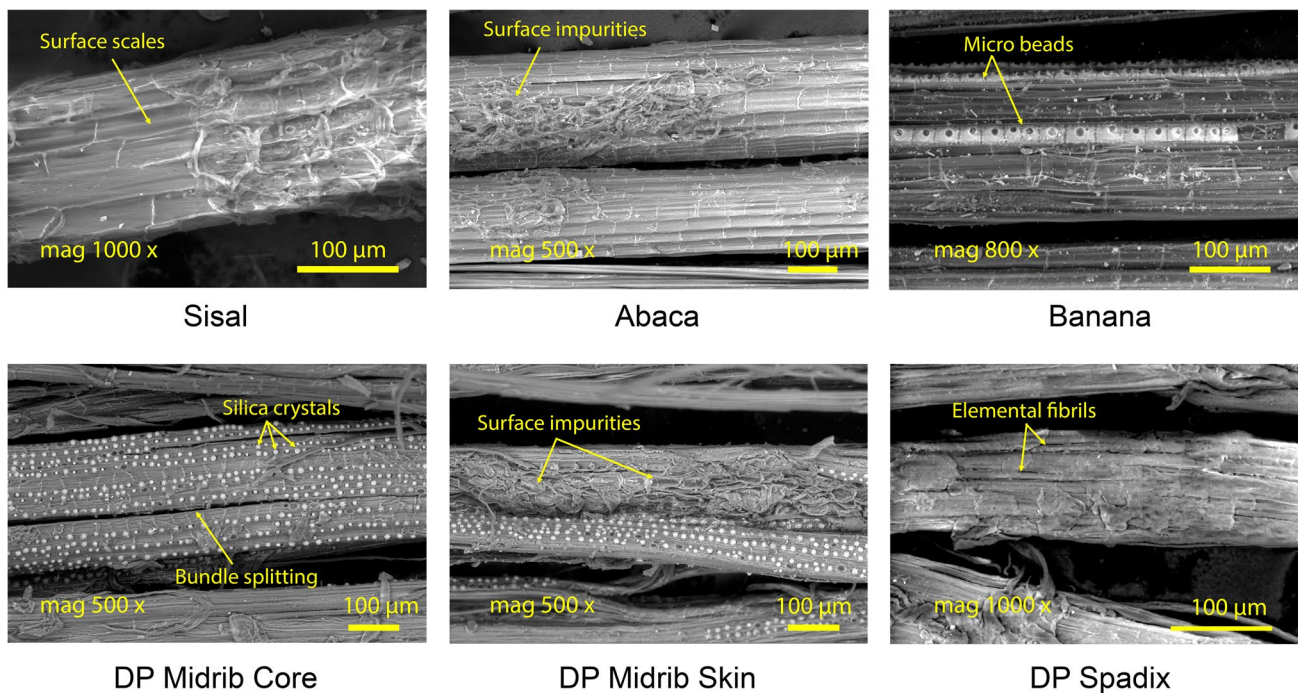


**Fig. 5** Longitudinal view of sisal, abaca, banana, DP midrib core and skin fibers, and DP spadix fibers

composite strength was nearly within the same range. This is due to the lower void content of date palm composites compared to sisal composites which resulted in better adhesion between fibers and matrix. Finally, the banana composite ( $15.78 \pm 3.13$  MPa) was the weakest among the other composites. This is due to the low strength of banana fibers ( $377.5 \pm 149$  MPa) and the presence of several air voids inside the banana composite as discussed earlier. Date palm composites have high tensile strength within the same range as sisal PP composites and even higher than banana composites by nearly 25%.

The strain at the break of the composites also followed the same trend as the fibers' failure strain. The average strain at break of the abaca composite was also the highest among the 6 other composites as shown in Fig. 4d. The strain at break of sisal composites ( $3.07 \pm 0.629\%$ ) and date palm midrib skin ( $2.34 \pm 0.67\%$ ) and date palm spadix ( $2.71 \pm 0.13\%$ ) composites were not statistically different. This is similar to the strain behavior of the fibers; the strain of sisal and DP spadix fibers were also within the same range. The strain at break of banana composite ( $2.32 \pm 0.087\%$ ) was within the same range as date palm midrib core and skin composites:  $2.09 \pm 0.134\%$  and  $2.34 \pm 0.67\%$  respectively.

As for the modulus of elasticity results, there was no statistical difference between all the average values except for banana fibers which were the lowest as shown in Fig. 4c. The tensile properties of the date palm composites are comparable to other composites reinforced with commercially

available fibers. The tensile behavior of the composites in this work is in agreement with the literature [14, 16, 17].

### 3.2.1 Tensile fracture surface

The morphology of the fractured surfaces of tensile specimens is shown in Fig. 6. The SEM micrographs show that the composites experienced fiber pull-out and debonding as a result of the tensile fracture. The presence of dry fibers inferred a reduction in bond strength between natural fibers and PP. All composites experienced fiber pull-out, debonding, and fiber fracture. According to Fig. 6, sisal and abaca composites had large areas of dry fibers and matrix discontinuity resulting in void creation.

### 3.3 Flexural properties

The bending strength of composites is affected by the in-plane tensile modulus of the composites. Hence, it is expected that the bending strength follows the same trend as the tensile modulus. However, the fiber diameter directly affects the flexural strength as well. As the fiber diameter increases, the resistant against bending increases. The equivalent diameter values of fibers are presented in Table 1. The typical bending stress–strain curves of the six composites and the average bending chord modulus values are shown in Fig. 7a and b respectively. After analyzing the tensile and the flexural data, it was expected that the bending strength of the sisal

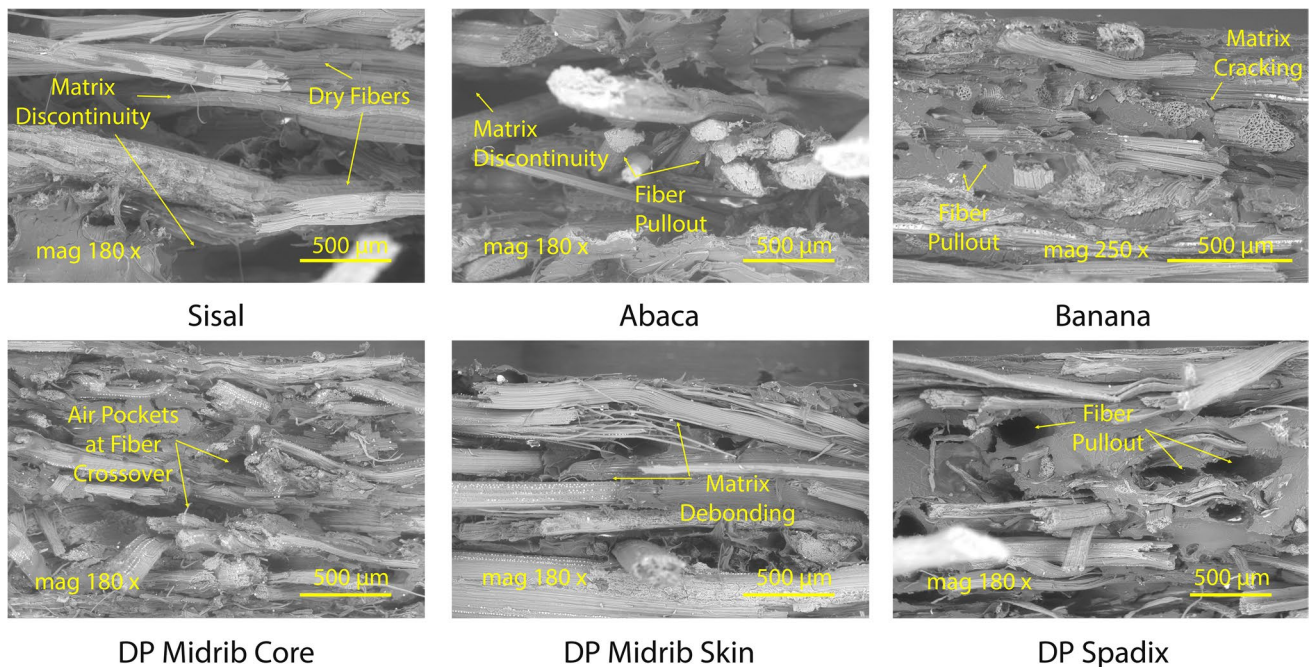


Fig. 6 SEM micrographs of the composite fractured surfaces



composite is higher than that of the abaca composites since the sisal composite has a higher tensile modulus. However, the abaca composite had higher average bending strength due to its larger fiber diameter/size. The same was observed between date palm midrib skin fibers, midrib core, and spadix fibers. The date palm midrib skin composite had higher bending strength than midrib core and spadix composites despite its lower tensile modulus, which was due to the large size of skin fibers compared to the other two fibers. In conclusion, sisal and abaca composites had the highest bending strength followed by date palm composites and finally banana which had the lowest bending strength. There was no statistical significance in flexural strength between all composites except for banana fibers as shown in Fig. 7b. As for the flexural chord modulus, it followed the same trend as the bending strength. The abaca composite had the highest modulus followed by sisal, midrib skin, midrib core, and spadix composites. Finally, banana composites had the lowest flexural chord modulus. Date palm PP composites have flexural properties comparable to PP composites reinforced with commercially available fibers such as sisal and abaca fibers. Date palm could be used in various applications and provide high durability. Additionally, the flexural properties of PP composites reinforced with bast fibers were comparable

to the results in this work. The jute PP composite had flexural strength of nearly 37.81 MPa [42], while in another study by Kandola et al. [14], the flexural strength and modulus of elasticity of jute PP composites were  $45.4 \pm 3.3$  MPa and  $3.7 \pm 0.2$  GPa. Bamboo PP composites have bending strength of nearly 53 MPa [43].

### 3.4 Impact properties

The impact test is considered a dynamic test which is different from the tensile and flexural tests which are considered quasi-static. The force applied to the specimens is in the form of a striker weight that is dropped on the specimens in a short period of time. The typical force–displacement curves of the six composite samples are presented in Fig. 8a. The initial part of the curves is due to the presence of discontinuities followed by the appearance of the first peak. This was followed by complex crack propagation due to debonding between fibers and matrix. The presence of a second peak in some of the cases is due to delamination. Afterwards, the curves start to gradually drop due to the resistance of the inner layers representing the penetration of the striker. The behavior of sisal and abaca composites was different from the other 4 composites. Full penetration occurred in the case

**Fig. 7** **a** Typical bending stress–strain curves and **b** average values of bending strength and modulus of rupture of the six fibers

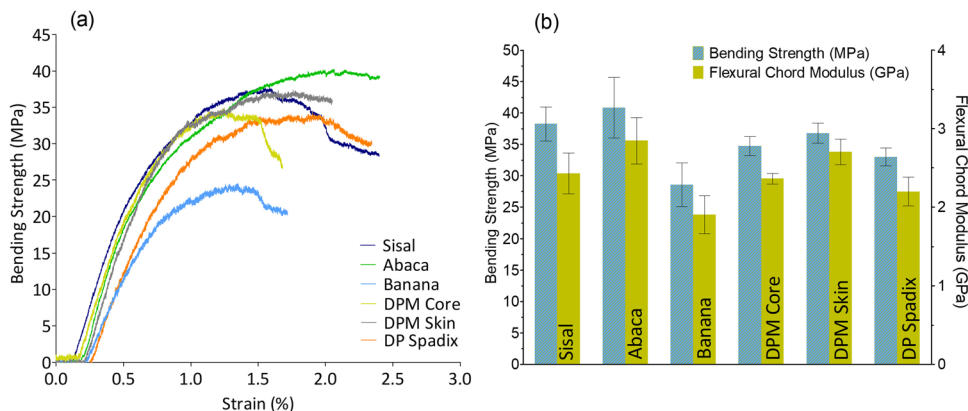
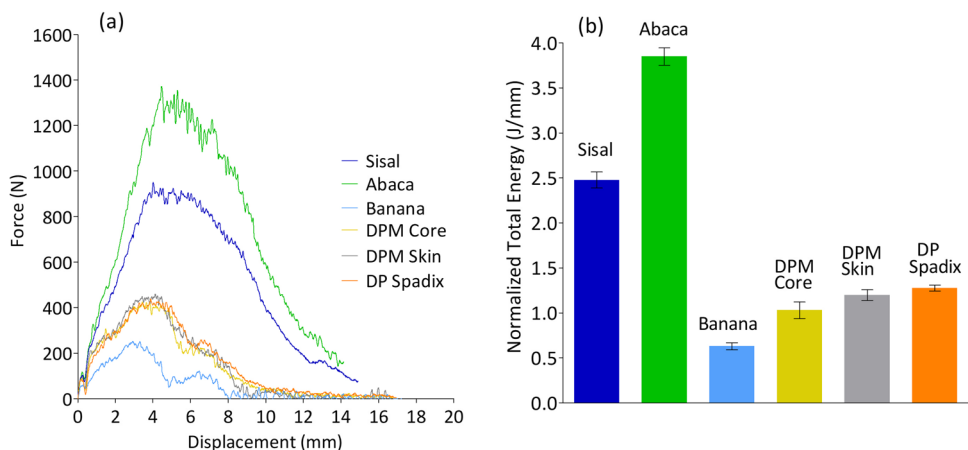


**Fig. 8** **a** Typical impact force–displacement curves and **b** normalized total energy of the six samples



of sisal and abaca composites which is confirmed by the fracture surfaces shown in Fig. 9. On the other hand, the force–displacement curves of date palm and banana composites imply gradual delamination of composites.

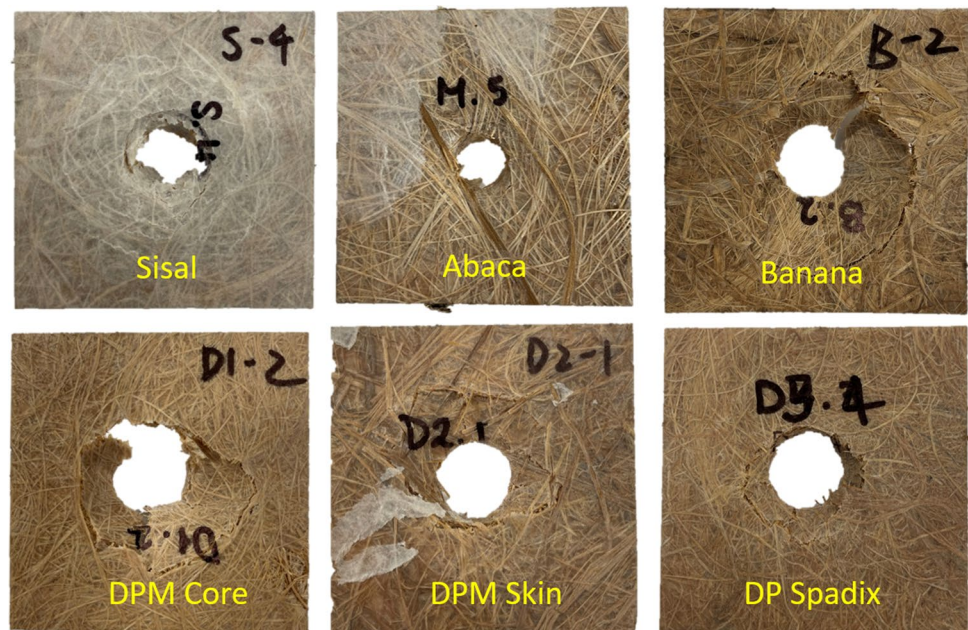
The total energy values of the composites depend greatly on the thickness. Therefore, for fair comparison, normalized total energy values were calculated by dividing the total energy by the composite thickness. The amount of energy absorbed during the test is related to the toughness of the fibers, the load-bearing element. Hence, as shown in Fig. 8b, abaca composites had the highest normalized total energy compared to the other 5 composites of  $3.85 \pm 0.097$  J/mm followed by sisal composites ( $2.48 \pm 0.088$  J/mm). Date palm core, skin, and spadix composites had normalized total energy values near each other:  $1.03 \pm 0.09$  J/mm,  $1.2 \pm 0.06$  J/mm, and  $1.28 \pm 0.038$  J/mm respectively. The normalized total energy of DPM skin composites was higher than that of DPM core fibers due to the large diameter of skin fibers. Finally, banana composites had the lowest normalized total energy values of  $0.63 \pm 0.04$  J/mm.

### 3.5 Dynamic mechanical analysis

DMA analysis is a test performed to determine the viscoelastic properties of composites. DMA analysis is essential to determine the properties of materials over a wide range of temperature. The storage modulus  $E'$ , referred to as dynamic modulus, is related to the composite's stiffness. The storage modulus is the ability of the material to store applied energy and it determines how stiff is the composite. The loss modulus  $E''$ , referred to as dynamic loss modulus, is the viscous response of the material. It is a measure of the

material ability to dissipate applied energy.  $E''$  values are very sensitive to the relaxation process and molecular mobility. Finally,  $\tan \delta$ , which is referred to as the mechanical damping factor, is a dimensionless parameter.  $\tan \delta$  is the ratio between the loss modulus and the storage modulus. As the value of  $\tan \delta$  decreases, it means that the material is highly elastic. On the other hand, high  $\tan \delta$  values mean that the material has high non-elastic strain [44]. Figure 10 shows the storage modulus, the loss modulus, and the  $\tan \delta$  curves for the six composites. During heating, the material goes from the glassy state to the rubbery state as shown in Fig. 10a. The storage modulus decreased with the increase in the temperature as shown in Fig. 10a. This could be due to the softening of the PP matrix caused by the heating effect [45, 46]. Table 3 shows the storage modulus values at temperatures in the glassy, glass transition, and rubbery regions. The increase in the storage modulus as in the case of abaca and DP midrib core composites is due to the restriction of PP mobility. Maximum loss modulus values in Fig. 10b correspond to heat dissipation due to the relaxation phenomenon.  $\tan \delta$  curves for the six composites are shown in Fig. 10c. There was not a huge difference between the damping behavior of the composites except a slight increase in the  $\tan \delta$  values of the banana and midrib skin composites. The first peak represents the glass transition temperature  $T_g$  and the second peak corresponds to the melting temperature  $T_m$ . The glass transition temperature was nearly around  $10^\circ\text{C}$ . Mechanical damping is affected by the fiber-matrix interfacial bond, frictional damping due to slippage or delamination, and damping due to defects in matrix and fibers [47]. The behavior of the composites is similar to other PP composites in the literature [45, 47–49]. From the literature,

**Fig. 9** Drop weight impact fracture surface



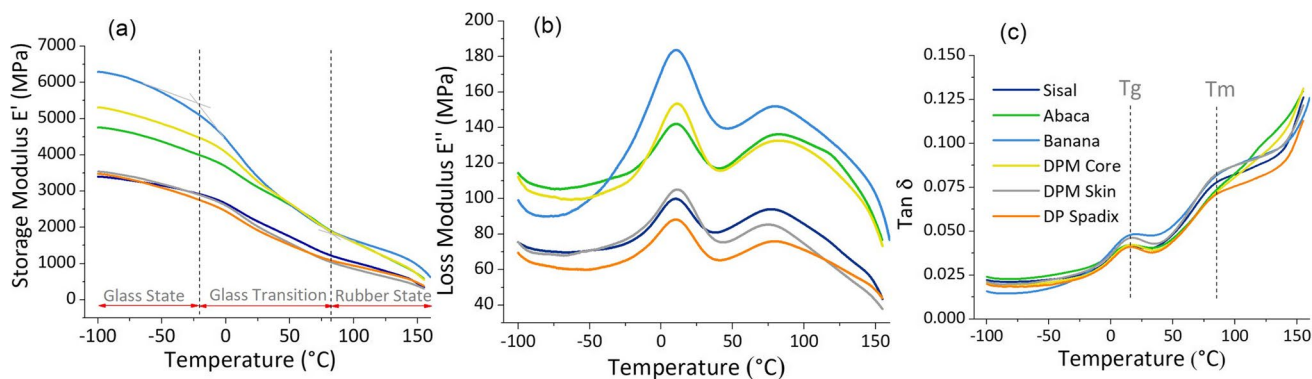


**Fig. 10** Relationship between **a** storage modulus, **b** loss modulus, and **c** Tan  $\delta$  versus temperature for the six composites

**Table 3** Storage modulus values of the six composites at various temperatures

Composite	Storage modulus (MPa)		
	At -50 °C	At 50 °C	At 125 °C
Sisal	3147.7	1733.02	792.8
Abaca	4377.4	2625.4	1154.1
Banana	5720.3	2605.8	1350
DPM core	4851.9	2666.7	1154.1
DPM skin	3204.3	1556.7	623.04
DP spadix	3147.7	1500.2	736.22

the storage modulus of 50% jute PP composite was nearly 4000 MPa at -50 °C. Additionally, the loss modulus and Tan  $\delta$  for the same composite at 0 °C were found to be nearly 140 MPa and less than 0.05 respectively [46].

### 3.6 Water absorption and thickness swelling

The results of the water absorption and thickness swelling are shown in Fig. 11. Water absorption in composites has three mechanisms. The first mechanism is due to water diffusion between micro gaps in the matrix. The second mechanism is due to capillary action between fibers and matrix due to poor interfacial bonds. Finally, the third mechanism is due to water transport in micro cracks appearing due to natural fiber swelling as a result of water storage [50]. Figure 11a shows the three water absorption mechanisms. The water absorption is affected by internal and external factors. The internal factors are mainly the fiber weight fraction, fibers' structure, fiber-matrix interfacial bond, void content, lumen size, and composite defects. The external factors are related to the test conditions such as the humidity and immersion water temperature. In this research work, only the effect of the internal factors on the results is discussed since all composites were tested under the same conditions. Figure 11b shows the percentage of water absorption

versus immersion time in distilled water. The maximum water absorption percentage was after 24 h of immersion. Afterwards, the composite weights were slightly increased linearly over the time. The water absorption of the sisal composite ( $33.6 \pm 5.6\%$ ) was the highest among the other six composites followed by abaca ( $20 \pm 2.6\%$ ) and banana ( $18.76 \pm 2.89\%$ ) composites. Date palm composites had the lowest water uptake compared to the other composites and had nearly the same water absorption percentages. Date palm spadix, midrib core, and midrib skin composites had water uptake values of  $12.3 \pm 1.4\%$ ,  $11.54 \pm 1\%$ , and  $13.76 \pm 2.9\%$  respectively. The water absorption of sisal and abaca composites is mostly because their thickness values are higher than the other composites and due to the high void content compared to the other composites as shown in Table 2. As mentioned earlier, the presence of voids in composites leads to high water absorption percentages. In spite of the small thickness of the banana composite, it had high water absorption wt.%. This is due to the poor fiber-matrix interfacial bond and the presence of voids in the banana composite (Fig. 6). The high water uptake values are due to the high fiber weight content. Kittikorn et al. [51] studied the effect of fiber weight fraction on the amount of water absorption. The results showed that the WA of composites reinforced with 40% fibers has absorbed 6 times the amount of water absorbed by composites that only have 20% fibers [18, 51]. The WA of hemp PP composites was between 20 and 25% after 24 h of immersion [18].

The thickness swelling results are shown in Fig. 11c. The factors that directly affect the thickness swelling are the void % and the cell wall thickness. As the amount of water in fibers increases, the cell wall of fibers absorbs more moisture through the formation of hydrogen bonds. Consequently, the cell walls swell significantly [52]. Figure 12 shows the effect of water absorption on the fiber swelling. The major increase in composites thickness was achieved after 24 h of immersion in distilled water. The date palm skin composite had the highest increase in thickness ( $19.4 \pm 5.8\%$ ) which

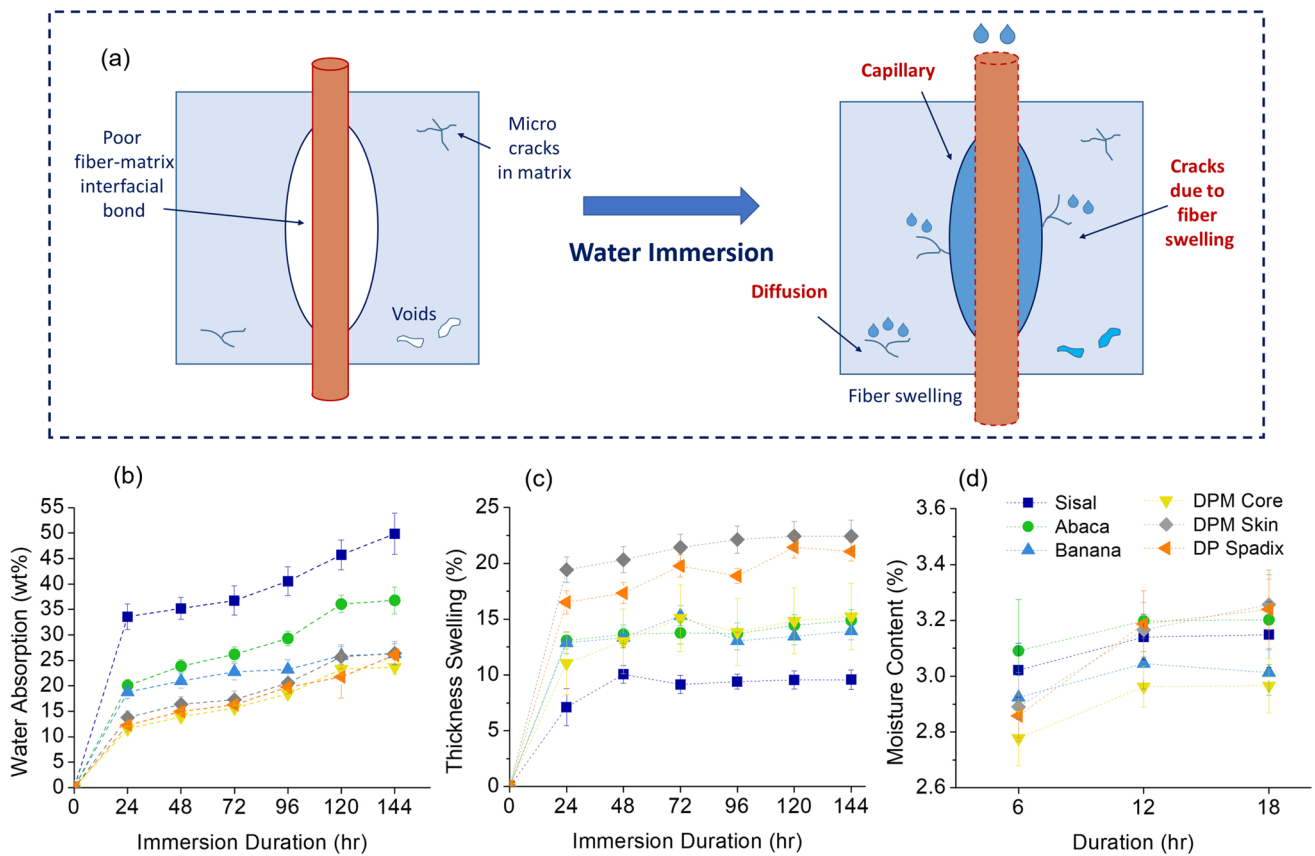
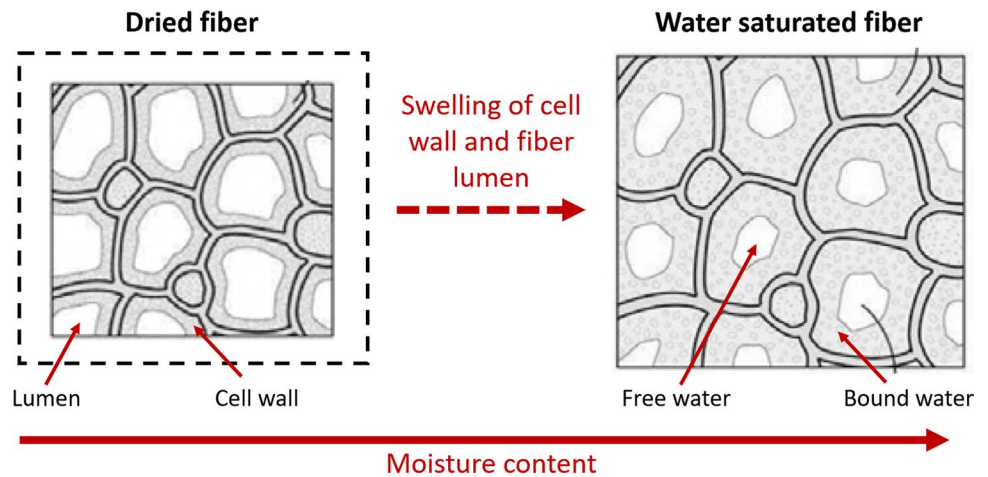


**Fig. 11** **a** Water absorption mechanisms, **b** water uptake percentage, **c** thickness swelling, and **d** moisture content weight percentage of the six composites vs. duration in hours

**Fig. 12** Natural fiber swelling mechanism



was followed by the spadix composite ( $16.5 \pm 5.23\%$ ). This is because the thickness of date palm fibril is larger than that of the other fibers. Hence, when the composites were immersed in water, the fibers swelled more due to cell wall moisture absorption. The lumen size contributes more to the amount of water absorbed. Abaca and banana composites had nearly the same thickness swelling:  $13.09 \pm 3.82\%$

and  $12.88 \pm 4.8\%$  respectively. The thickness swelling of the midrib core composite was nearly  $11.05 \pm 4.15\%$  after 24 h of water immersion. Finally, the sisal composite had the lowest increase in thickness ( $7.11 \pm 8.13\%$ ) compared to the other six composites.

The moisture content results are shown in Fig. 11d. Nearly all composites had the same moisture wt.% before the

**Table 4** Comparison between this work and automotive FlexForm panels [53] based on average values

PP%/NF%	Thickness (mm)	Areal density (gm/m <sup>2</sup> )	Tensile		Flexural		Impact		Water absorption after 24 h (%)
			Strength (MPa)	Modulus (GPa)	Strength (MPa)	Modulus (GPa)	Peak load (N/mm)	Total energy (J/mm)	
		ASTM D3776	ASTM D3039	ASTM D3039	ASTM D790	ASTM D790	ASTM D3763	ASTM D3763	BS EN 322
50/50 sisal	2.7	1815	23.52	2.93	38.2	2.43	954.2	7.5	33.6
50/50 abaca	2.6	1815	31	2.74	40.84	2.85	1337.5	9.9	20
50/50 banana	1.94	1488	16.2	2.07	28.6	1.9	262.4	1.22	18.8
50/50 DPM core	2	1694	21.1	2.93	34.7	2.4	430.05	2.2	11.58
50/50 DPM skin	2.1	1730	20.74	2.23	36.8	2.7	479.4	2.6	13.8
50/50 DP spadix	1.9	1597	22.4	2.47	33.0	2.2	426.2	2.5	12.3
FlexForm 50PP/50NF [53]	1.95	1600	24.13	-	-	2.6	-	-	25
FlexForm 50PP/50NF [53]	2.2	1800	27	-	-	2.55	-	-	25

first drying cycle around 3 wt.%. The date palm core composite had the lowest moisture content of  $2.78 \pm 0.2$  wt.% while the abaca composite had the highest moisture content of nearly  $3.09 \pm 0.4$  wt.%. After 12 h of heating, the moisture content in the six composites dropped to less than 0.5 wt.%.

## 4 Benchmarking

The composites in this work were manufactured according to the automotive standards. Table 4 compares between the manufactured composites and FlexForm Technologies (Elkhart, USA) 50PP/50NF panels. The properties of date palm composites were near the properties of FlexForm panels having 1600 gm/m<sup>2</sup> areal density. The water absorption properties of all composites in this work were better than FlexForm composites except for sisal composites. By manufacturing process optimization, leaf fiber composites including date palm have a high potential in being used in the automotive industry.

## 5 Conclusion

The purpose of this work was to benchmark the composites reinforced with a new class of natural fibers obtained from date palm against other PP composites reinforced with commercial leaf fibers. The results showed that date palm fibers have competitive properties and high potential availability. The tensile strength of DP composites was within the same range as sisal composites with no significant difference, while the tensile modulus of the DP midrib core composite was similar to the abaca composite.

The flexural properties of the DP composites were similar to abaca and sisal composites. Additionally, the water absorption percentage of DP composites was much lower than the other three composites. The WA% of sisal and abaca composites were higher than DP composites by nearly 70% and 50% respectively. The DMA results showed that DP composites have storage and loss moduli values comparable to the other three composites. The valorization of date palm fibers may increase the biodiversity of natural fibers and provide the composite industry with a new sustainable fiber reinforcement. As per our knowledge, this work is considered the first attempt to manufacture nonwoven composites from long textile date palm fibers. The results obtained in this work are very promising and highlight the points of strength of date palm fibers and their composites. Date palm fibers are still in their embryonic stage, and with further research and development, the fibers can reach new horizons to help support the regional transition towards the circular bioeconomy of the future.

**Acknowledgements** The authors would like to thank the Canal Rope company and El Nidaa Foundation for providing the sisal, abaca, and banana fibers. Also, the authors are thankful to Dr. Ang Li, a post-doctoral researcher, for his help in performing the drop weight impact testing at the composite core facility at the Wilson College of Textiles in North Carolina State University.

**Author contribution** All authors wrote the main manuscript text and prepared the figures. All authors reviewed the manuscript.

**Funding** Open access funding provided by The Science, Technology & Innovation Funding Authority (STDF) in cooperation with The Egyptian Knowledge Bank (EKB).

**Data availability** The data used during this study is available and can be presented upon request.

## Declarations

**Ethics approval and consent to participate** Not applicable.

**Consent for publication** Not applicable.

**Competing interests** The authors declare no competing interests.

**Open Access** This article is licensed under a Creative Commons Attribution 4.0 International License, which permits use, sharing, adaptation, distribution and reproduction in any medium or format, as long as you give appropriate credit to the original author(s) and the source, provide a link to the Creative Commons licence, and indicate if changes were made. The images or other third party material in this article are included in the article's Creative Commons licence, unless indicated otherwise in a credit line to the material. If material is not included in the article's Creative Commons licence and your intended use is not permitted by statutory regulation or exceeds the permitted use, you will need to obtain permission directly from the copyright holder. To view a copy of this licence, visit <http://creativecommons.org/licenses/by/4.0/>.

## References

- Orsato RJ, Wells P (2007) U-turn: the rise and demise of the automobile industry. *J Clean Prod* 15:994–1006. <https://doi.org/10.1016/j.jclepro.2006.05.019>
- ICCT (2017) Fact sheet: Footprint versus mass: how to best account for weight reduction in the European vehicle co 2 regulation
- Fontaras G, Zacharof N-G, Ciuffo B (2017) Fuel consumption and CO<sub>2</sub> emissions from passenger cars in Europe - laboratory versus real-world emissions. *Prog Energy Combust Sci* 60:97–131. <https://doi.org/10.1016/j.pecs.2016.12.004>
- Suddell BC, Evans WJ (2005) Natural fiber composites in automotive applications. In: Mohanty AK, Misra M, Drzal LT (eds) *Natural fibers, biopolymers, and biocomposites*. Taylor & Francis, pp 231–259
- Akampunguzo O, Wambua PM, Ahmed A et al (2017) Review of the applications of biocomposites in the automotive industry. *Polym Compos* 38:2553–2569. <https://doi.org/10.1002/pc.23847>
- Mann GS, Singh LP, Kumar P, Singh S (2018) Green composites: a review of processing technologies and recent applications. *J Thermoplast Compos Mater*. <https://doi.org/10.1177/0892705718816354>
- Suddell BC (2008) Industrial fibres: recent and current developments. *Proc Symp Nat Fibres* 44:71–82
- Elseify LA, Midani M, El-Badawy A, Jawaid M (2021) Natural fiber composite qualification in the automotive industry. In: *Manufacturing automotive components from sustainable natural fiber composites*, 1st ed. Springer Nature, pp 53–65
- Ibrahim H, Mehanny S, Darwish L, Farag M (2017) A comparative study on the mechanical and biodegradation characteristics of starch-based composites reinforced with different lignocellulosic fibers. *J Polym Environ* 0:1–14. <https://doi.org/10.1007/s10924-017-1143-x>
- Prajwal B, Giridharan BV, Vamshi KK et al (2019) Sisal fiber reinforced polypropylene bio-composites for inherent applications. *Int J Recent Technol Eng* 8:305–309
- Ochi S (2006) Development of high strength biodegradable composites using Manila hemp fiber and starch-based biodegradable resin. *Compos Part A Appl Sci Manuf* 37:1879–1883. <https://doi.org/10.1016/j.compositesa.2005.12.019>
- Arya A, Tomlal JE, Gejo G, Kuruvilla J (2015) Commingled composites of polypropylene/coir-sisal yarn: effect of chemical treatments on thermal and tensile properties. *E-Polymers* 15:169–177. <https://doi.org/10.1515/epoly-2014-0186>
- Bledzki AK, Franciszczak P, Osman Z, Elbadawi M (2015) Polypropylene biocomposites reinforced with softwood, abaca, jute, and kenaf fibers. *Ind Crops Prod* 70:91–99. <https://doi.org/10.1016/j.indcrop.2015.03.013>
- Kandola BK, Mistik SI, Pornwannachai W, Anand SC (2018) Natural fibre-reinforced thermoplastic composites from woven-nonwoven textile preforms: Mechanical and fire performance study. *Compos Part B Eng* 153:456–464. <https://doi.org/10.1016/j.compositesb.2018.09.013>
- Motaleb KZMA, Ahad A, Laureckiene G, Milasius R (2021) Innovative banana fiber nonwoven reinforced polymer composites: pre- and post-treatment effects on physical and mechanical properties. *Polymers (Basel)* 13. <https://doi.org/10.3390/polym13213744>
- Ng LF, Dhar Malingam S, Selamat MZ et al (2020) A comparison study on the mechanical properties of composites based on kenaf and pineapple leaf fibres. *Polym Bull* 77:1449–1463. <https://doi.org/10.1007/s00289-019-02812-0>
- Anuar NIS, Zakaria S, Gan S et al (2019) Comparison of the morphological and mechanical properties of oil palm EFB fibres and kenaf fibres in nonwoven reinforced composites. *Ind Crops Prod* 127:55–65. <https://doi.org/10.1016/j.indcrop.2018.09.056>
- Hargitai H, Rác I, Anandjiwala R (2006) Development of hemp fibre - PP nonwoven composites. *Macromol Symp* 239:201–208. <https://doi.org/10.1002/masy.200690097>
- Elseify LA, Midani M, Shihata LA, El-Mously H (2019) Review on cellulosic fibers extracted from date palms (*Phoenix Dactylifera L.*) and their applications. *Cellulose* 26:2209/2232. <https://doi.org/10.1007/s10570-019-02259-6>
- Wazzan AA (2006) Effect of fiber orientation on the mechanical properties and fracture characteristics of date palm fiber reinforced composites. *Int J Polym Mater* 54:213–225. <https://doi.org/10.1080/00914030390246379>
- Tripathy S, Dehury J, Mishra D (2016) A study on the effect of surface treatment on the physical and mechanical properties of date-palm stem fiber embedded epoxy composites. *IOP Conf Ser Mater Sci Eng* 115:012036. <https://doi.org/10.1088/1757-899X/115/1/012036>
- Sadik T, Sivaram NM, Senthil P (2017) Evaluation of mechanical properties in date palm fronds polymer composites. *Int J ChemTech Res* 10:558–564. <https://doi.org/10.1063/1.5085592>
- Alawar A, Hamed AM, Al-Kaabi K (2008) Date palm tree fiber as polymeric matrix reinforcement, DPF-polypropylene composite characterization. *Adv Mater Res* 47–50:193–196. <https://doi.org/10.4028/www.scientific.net/AMR.47-50.193>
- Mahdavi S, Kermanian H, Varshoei A (2010) Comparison of mechanical properties of date palm fiber-polyethylene composite. *BioResources* 5:2391–2403. <https://doi.org/10.15376/biores.5.4.2391-2403>
- Sbiai A (2010) Short date palm tree fibers/polyepoxy composites prepared using RTM process: effect of tempo mediated oxydation of the fibers. *BioResources* 5:672–689
- Al-Sulaiman FA (2002) Mechanical properties of date palm fiber reinforced composites. *Appl Compos Mater* 9:369–377. <https://doi.org/10.1023/A:1020216906846>
- Hammood AS (2015) Effect of erosion on water absorption and morphology for treated date palm fiber-reinforced polyester composites. *Int J Mech Mechatronics Eng* 15:108–114
- Supian ABM, Jawaid M, Rashid B et al (2021) Mechanical and physical performance of date palm/bamboo fibre reinforced epoxy hybrid composites. *J Mater Res Technol* 15:1330–1341. <https://doi.org/10.1016/j.jmrt.2021.08.115>

29. Refaai MRA, Reddy RM, Reddy MI, et al (2022) Investigation on physical and mechanical characteristics of date palm fiber reinforced aliphatic epoxy hybrid composites. *Adv Polym Technol* 2022:11. <https://doi.org/10.1155/2022/4916499>
30. Abdellah MY, Seleem A-EHA, Marzok WW, et al (2022) Tensile and fracture properties of hybrid date palm fibre composite structures embedded with chopped rubber. *Int J Eng Res Appl* 12:54–66. <https://doi.org/10.9790/9622-1205015466>
31. Ghori SW, Rao GS, Rajhi AA (2022) Investigation of physical, mechanical properties of treated date palm fibre and kenaf fibre reinforced epoxy hybrid composites. *J Nat Fibers* 20:12. <https://doi.org/10.1080/15440478.2022.2145406>
32. Jawaid M, Awad S, Fouad H et al (2021) Improvements in the thermal behaviour of date palm/bamboo fibres reinforced epoxy hybrid composites. *Compos Struct* 277:114644. <https://doi.org/10.1016/j.compstruct.2021.114644>
33. Ali M (2023) Epoxy – date palm fiber composites: study on manufacturing and properties. *Int J Polym Sci* 2023:12. <https://doi.org/10.1155/2023/5670293>
34. Djoudi T, Hecini M, Scida D et al (2019) Physico-mechanical characterization of composite materials based on date palm tree fibers. *J Nat Fibers* 0:1–14. <https://doi.org/10.1080/15440478.2019.1658251>
35. Mirmehdi SM, Zeinaly F, Dabbagh F (2014) Date palm wood flour as filler of linear low-density polyethylene. *Compos Part B Eng* 56:137–141. <https://doi.org/10.1016/j.compositesb.2013.08.008>
36. Ali ME, Alabdulkarem A (2017) On thermal characteristics and microstructure of a new insulation material extracted from date palm trees surface fibers. *Constr Build Mater* 138:276–284. <https://doi.org/10.1016/j.conbuildmat.2017.02.012>
37. Saleh MA, Al Haron MH, Saleh AA, Farag M (2017) Fatigue behavior and life prediction of biodegradable composites of starch reinforced with date palm fibers. *Int J Fatigue* 103:216–222. <https://doi.org/10.1016/j.ijfatigue.2017.06.005>
38. Saba N, Allothman OY, Almutairi Z et al (2019) Date palm reinforced epoxy composites: tensile, impact and morphological properties. *J Mater Res Technol* 8:3959–3969. <https://doi.org/10.1016/j.jmrt.2019.07.004>
39. Mathijssen D (2021) The challenging path to add a promising new bio-fiber from an overlooked source to our reinforcement toolbox: Date palm fibers. *Reinf Plast* 65:48–52. <https://doi.org/10.1016/j.repl.2020.12.004>
40. Midani M, Elseify LA, Hassanin A, Hamouda T (2021) Egyptian consortium develops first textile palm fibres and reinforcements. *JEC Compos* 138:52–53
41. Elseify LA, Midani M, El-Badawy AA et al (2022) Comparative study of long date palm (*Phoenix Dactylifera* L.) midrib and spadix fibers with other commercial leaf fibers. *Cellulose* 30:1927–1942. <https://doi.org/10.1007/s10570-022-04972-1>
42. Bera M, Alagirusamy R, Das A (2010) A study on interfacial properties of jute-PP composites. *J Reinf Plast Compos* 29:3155–3161. <https://doi.org/10.1177/0731684410369723>
43. Tang Q, Wang Y, Wang G, et al (2019) An investigation on the comprehensive property assessment and future directions of single bamboo fiber reinforced polypropylene composites fabricated by a non-woven paving and advanced molding process. *Materials (Basel)* 12:13. <https://doi.org/10.3390/ma12162641>
44. Saba N, Jawaid M, Allothman OY, Paridah MT (2016) A review on dynamic mechanical properties of natural fibre reinforced polymer composites. *Constr Build Mater* 106:149–159. <https://doi.org/10.1016/j.conbuildmat.2015.12.075>
45. Karaduman Y, Sayeed MMA, Onal L, Rawal A (2014) Viscoelastic properties of surface modified jute fiber/polypropylene nonwoven composites. *Compos Part B Eng* 67:111–118. <https://doi.org/10.1016/j.compositesb.2014.06.019>
46. George G, Tomlal Jose E, Åkesson D et al (2012) Viscoelastic behaviour of novel commingled biocomposites based on polypropylene/jute yarns. *Compos Part A Appl Sci Manuf* 43:893–902. <https://doi.org/10.1016/j.compositesa.2012.01.019>
47. John MJ, Anandjiwala RD (2009) Chemical modification of flax reinforced polypropylene composites. *Compos Part A Appl Sci Manuf* 40:442–448. <https://doi.org/10.1016/j.compositesa.2009.01.007>
48. Hong CK, Kim N, Kang SL et al (2008) Mechanical properties of maleic anhydride treated jute fibre/polypropylene composites. *Plast Rubber Compos* 37:325–330. <https://doi.org/10.1179/174328908X314334>
49. Shaikh H, Allothman OY, Alshammari BA, Jawaid M (2023) Dynamic and thermo-mechanical properties of polypropylene reinforced with date palm nano filler. *J King Saud Univ - Sci* 35:102561. <https://doi.org/10.1016/j.jksus.2023.102561>
50. Arman NSN, Chen RS, Ahmad S (2021) Review of state-of-the-art studies on the water absorption capacity of agricultural fiber-reinforced polymer composites for sustainable construction. *Constr Build Mater* 302:124174. <https://doi.org/10.1016/j.conbuildmat.2021.124174>
51. Kittikorn T, Ek M, Karlsson S (2013) Comparison of water uptake as function of surface modification of empty fruit comparison of water uptake as function of surface modification of empty fruit bunch oil palm fibres in. *BioResources* 8:2998–3016. <https://doi.org/10.15376/biores.8.2.2998-3016>
52. Garat W, Le Moigne N, Corn S et al (2020) Swelling of natural fibre bundles under hygro- and hydrothermal conditions: determination of hydric expansion coefficients by automated laser scanning. *Compos Part A Appl Sci Manuf* 131:105803. <https://doi.org/10.1016/j.compositesa.2020.105803>
53. FlexForm (2013) FlexForm technologies: the leader in natural fiber composites

**Publisher's note** Springer Nature remains neutral with regard to jurisdictional claims in published maps and institutional affiliations.